Electron-loss and excitation cross sections for a He^+ ion colliding with various atoms

Toshiaki Kaneko
Department of Applied Physics, Okayama University of Science, Ridai-cho 1-1, Okayama 700, Japan
(Received 25 September 1984; revised manuscript received 15 May 1985)

A unitarized impact-parameter method is applied to calculate the electron-loss and excitation cross sections for He^+ ions colliding with atoms. The projectile ionization and excitation are dominantly caused by the average potential field of the target atom (atomic number Z_2). The inelastic process of exciting the target atom contributes negligibly except for light target elements. We adopt the Molière potential to describe this average potential field. The energy dependences of the electron-loss cross sections in He, N_2, and Ar targets are in good agreement with the reported data. In the case of the Kr target, the present theory yields larger cross sections than the data, especially below 1 MeV impact energy of a He^+ projectile. The calculated loss cross sections at impact velocity ranging from $2v_0$ to $6v_0$ ($v_0=2.18\times10^8$ cm/s) show a weaker Z_2 dependence in the large Z_2 region than that given by the Bohr formula. As for the cross section for exciting the ground state of a projectile to the first excited state, a similar weak Z_2 dependence can be found. The recent experimental results using 40-MeV F^{8+} ions colliding with He, Ne, Ar, and Kr targets have supported this tendency.

I. INTRODUCTION

In the ion-beam—material interaction, the problem of charge states of incident ions passing through matter has been studied intensively. In order to determine the charge-state distribution[1] and to investigate the charge-changing effect of impinging ions both on the energy loss[2] and on the energy straggling[3] for energetic ions, the data of the cross sections for electron loss and capture play an essential role. Moreover, the energy and material dependence of these cross sections is of great interest for a systematic and comprehensive understanding of atomic collisions in matter, including in solids.

As for a helium-ion beam, a large amount of the energy-loss data has been compiled[4] since it is a basic quantity to analyze the depth profiles of impurity atoms using the Rutherford backscattering method (RBS). The effective charge in the stopping phenomena, which is interpreted as the effective charge that a heavy ion has acquired through the resultant excitation of electrons in matter, is a useful quantity to arrange and predict the stopping-power data for heavy ions. Recently the average charge of helium ions with $\sim$MeV energies, obtained from the charge-state distribution, has been reasonably related to the effective charge,[5] where the experimental data reveal a strong Z_2 (target atomic number) oscillation in the average charge.[6,7] This effect can be explained theoretically by the fact that the electron-capture cross section for a He^{2+} ion displays the oscillating behavior with respect to Z_2 while the electron-loss cross section for a He^+ ion remains monotonic.[7,8] In order to calculate the electron-loss cross section in atomic collisions, the first Born approximation (FBA) is widely used, where we have to estimate the contributions independently from two cases. One case is that a target atom is excited and the other case is that it remains in the ground state in a collision. These two cases are referred to in this paper as the inelastic part and the elastic part, respectively. Judging from the elastic part contribution,[8] the electron-loss cross section for a He^+ ion is nearly proportional to Z_2^2 for small-Z_2 targets, while for large-Z_2 ones it depends on Z_2 more weakly since the target electrons screen the electric field provided by the nucleus. There are qualitative agreements with the data in the Z_2 dependence of the loss cross section. Quantitatively, however, there are non-negligible differences except for small-Z_2 atoms. This seems to imply that the FBA breaks down around the velocity $v\sim Z_1v_0$ (Z_1 is the atomic number of a projectile), where the loss cross section is maximum. Nevertheless, the FBA is actually of great use in treating excitation and ionization processes, since the closure expression and a scaling law for the cross sections are available.[9,10] It is not, however, quantitatively satisfactory for low impact energies (or velocities). On the other hand, based on the free-collision approximation, Bohr[11] estimated the loss cross section for an ion colliding with heavy atom at a high velocity v to be

$$\sigma_{\rm loss}=\pi a_0^2 Z_2^{2/3}(v_0/v)(I_0/I)^{1/2} \quad \text{for } v/v_0>(I/I_0)^{1/2}\ , \tag{1.1}$$

where $v_0=2.18\times10^8$ cm/s, $a_0=0.529\times10^{-8}$ cm, $I_0=13.6$ eV, and I denotes the binding energy of an ejected electron in eV. This formula has a different velocity dependence from the asymptotic velocity dependence of the FBA, and has presented at least qualitative agreement with data.

The aim of this paper is to give more satisfactory dependences of the loss cross section for He^+ ions on the physical parameters v and Z_2 over wide ranges. At the same time some new aspects in the investigation of the excitation cross section for He^+ projectiles with respect to Z_2 are also presented. In Sec. II, our calculation formulas are described, and Sec. III is devoted to present numerical

results and discussions. The atomic units ($e=m=\hbar=1$) are used throughout the paper unless otherwise stated, where the velocity and the length are measured in units of the Bohr velocity v_0 and the Bohr radius a_0, respectively.

II. FORMULATION

Let us consider the collision system composed of a projectile with one electron and a neutral target atom with Z_2 electrons. The position vectors of electrons from the nuclei are denoted by $\mathbf{r}_1$ and $\mathbf{r}_{2j}$ ($j=1,2,\ldots,Z_2$) (see Fig. 1). The extension of the theory for a projectile with more electrons is straightforward. We assume that a projectile moves with the constant velocity $\mathbf{v}$ on a straight-line trajectory with impact parameter b. Therefore the relative position vector $\mathbf{R}$ of the projectile from the nucleus of the target atom is described as

$$\mathbf{R}=\mathbf{v}t+\mathbf{e}_y b \ , \tag{2.1}$$

where $\mathbf{e}_y$ is the unit vector perpendicular to $\mathbf{v}$, and t denotes the time chosen such that the internuclear distance R is a minimum at $t=0$. Once the probability $\mathscr{P}(b)$ for a given reaction as a function of impact parameter b can be obtained, the cross section σ is calculated directly from the following:

$$\sigma=2\pi\int_0^\infty db\, b\,\mathscr{P}(b) \ . \tag{2.2}$$

The total Hamiltonian H of our system is written as

$$\begin{aligned}
&H=H_p+H_t+V_{\rm int}(t) \ , \\
&H_p=-\tfrac{1}{2}\Delta_1-Z_1/r_1 \ , \\
&H_t=\sum_k(-\tfrac{1}{2}\Delta_{2k}-Z_2/r_{2k})+\tfrac{1}{2}\sum_{k(\neq j)}1/|\mathbf{r}_{2k}-\mathbf{r}_{2j}| \ , \\
&V_{\rm int}(t)=-Z_2/|\mathbf{R}+\mathbf{r}_1|-\sum_j Z_1/|\mathbf{R}-\mathbf{r}_{2j}| \\
&\qquad\qquad +\sum_j 1/|\mathbf{r}_1-\mathbf{r}_{2j}+\mathbf{R}| \ ,
\end{aligned} \tag{2.3}$$

where H_p, H_t, and $V_{\rm int}(t)$ represent the Hamiltonian for the electron in the projectile, that for electrons in the target atom, and the interaction Hamiltonian between two-electron systems, respectively. And Δ_α ($\alpha=1,2k$) denotes the Laplacian operator with respect to r_α, where r_{2k} represents the position vector of the kth electron on nucleus 2 (the target nucleus). The time dependence of $V_{\rm int}(t)$ is introduced through the position vector $\mathbf{R}=\mathbf{R}(t)$. The wave function for the electron is governed by the time-dependent Schrödinger equation as follows:

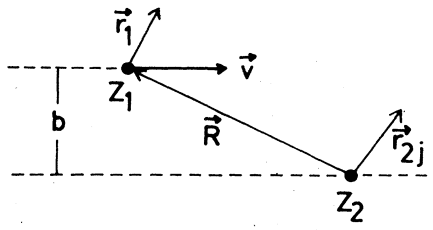

FIG. 1. Schematic of the coordinate system.

$$i\frac{\partial\psi}{\partial t}=H\psi \ . \tag{2.4}$$

According to the usual procedure, the wave function is expanded in terms of the linear combination of the product of eigenfunctions for the electrons both in the projectile and in the target atom such as

$$\begin{aligned}
&\psi(t)=\sum_{n,k}a_{nk}(t)\phi_n(\mathbf{r}_1)e^{-i\epsilon_n^{(p)}t}\Psi_k(\{\mathbf{r}_2\})e^{-i\epsilon_k^{(t)}t} \ , \\
&H_p\phi_n=\epsilon_n^{(p)}\phi_n, \quad H_t\Psi_k=\epsilon_k^{(t)}\Psi_k \ ,
\end{aligned} \tag{2.5}$$

where $\{\mathbf{r}_2\}$ stands for a set of the coordinates of the target electrons, and $\epsilon_n^{(p)}$ and $\epsilon_k^{(t)}$ the eigenenergies of electronic states labeled n and k, respectively. The subscripts (p) and (t) refer to "projectile" and "target," and $a_{nk}(t)$ is the expansion coefficient. Continuous states as well as discrete ones are denoted by n and k, symbolically.

Using (2.3)—(2.5), we get the following equation:

$$\begin{aligned}
i\frac{\partial a_{nk}(t)}{\partial t}&=\sum_{n',k'}\langle n;k\,|\,V_{\rm int}(t)\,|\,n';k'\rangle \\
&\quad\times\exp[i(\epsilon_{nk}-\epsilon_{n'k'})t]a_{n'k'}(t) \ ,
\end{aligned} \tag{2.6}$$

with

$$\begin{aligned}
&\langle n;k\,|\,V_{\rm int}(t)\,|\,n';k'\rangle \\
&\qquad=\int dr_1\int\prod_j dr_{2j}\phi_n^*\Psi_k^*V_{\rm int}(t)\phi_{n'}\Psi_{k'} \ ,
\end{aligned} \tag{2.7}$$

$$\epsilon_{nk}=\epsilon_n^{(p)}+\epsilon_k^{(t)} \ .$$

In order to eliminate the matrix element $\langle n;k\,|\,V_{\rm int}(t)\,|\,n;k\rangle$ in (2.6), the transformation is made

$$a_{nk}(t)=A_{nk}(t)\exp\left[-\int_{-\infty}^t dt'\langle n;k\,|\,V_{\rm int}(t')\,|\,n;k\rangle\right] . \tag{2.8}$$

Then the differential equation (2.6) is equivalent to

$$\begin{aligned}
i\frac{\partial A_{nk}(t)}{\partial t}&=\sum_{n',k'}\exp\left[i\int_{-\infty}^t dt'\langle n;k\,|\,V_{\rm int}(t')\,|\,n;k\rangle\right] \\
&\quad\times\{\langle n;k\,|\,V_{\rm int}(t)\,|\,n';k'\rangle\exp[i(\epsilon_{nk}-\epsilon_{n'k'})t]-\langle n;k\,|\,V_{\rm int}(t)\,|\,n;k\rangle\delta_{nn'}\delta_{kk'}\} \\
&\quad\times\exp\left[-i\int_{-\infty}^t dt''\langle n';k'\,|\,V_{\rm int}(t'')\,|\,n';k'\rangle\right]A_{n'k'}(t) \ ,
\end{aligned} \tag{2.9}$$

where δ_{ij} denotes the Kronecker delta. The above equation can be rewritten as

$$i\frac{\partial A_{nk}(t)}{\partial t}+\sum_{n',k'}\langle n;k\mid\tilde{V}(t)\mid n';k'\rangle A_{n'k'}(t)\ , \tag{2.10}$$

with

$$\tilde{V}(t)=\exp[i\gamma(t)][V_{\rm int}(t)-V_{{\rm int},d}(t)]\exp[-i\gamma(t)]\ , \tag{2.11}$$

where the matrix elements of the operators $\gamma(t)$ and $V_{{\rm int},d}(t)$ are given as follows:

$$\begin{aligned}&\langle n;k\mid\gamma(t)\mid n';k'\rangle=\left[\int_{-\infty}^{t}dt'\langle n;k\mid V_{\rm int}(t')\mid n;k\rangle+\epsilon_{nk}t\right]\delta_{nn'}\delta_{kk'}\ ,\\&\langle n;k\mid V_{{\rm int},d}(t)\mid n';k'\rangle=\langle n;k\mid V_{\rm int}(t)\mid n;k\rangle\delta_{nn'}\delta_{kk'}\ .\end{aligned} \tag{2.12}$$

In (2.11), $\tilde{V}(t)$ has vanishing diagonal matrix element $\langle n;k\mid\tilde{V}(t)\mid n;k\rangle$. The differential equation (2.10) is straightforwardly converted into the following integral equation:

$$A_{nk}(t)=\delta_{n0}\delta_{k0}-i\sum_{n',k'}\int_{-\infty}^{t}dt'\langle n;k\mid\tilde{V}(t')\mid n';k'\rangle A_{n'k'}(t')\ . \tag{2.13}$$

The probability of transition from the initial state $\mid 0;0\rangle$ to the final state $\mid n;k\rangle$ can be obtained as a function of the impact parameter such that

$$\mathscr{P}_{nk}(b)=\mid a_{nk}(\infty)\mid^2=\mid A_{nk}(\infty)\mid^2\ . \tag{2.14}$$

Using the iteration in (2.13), the transition amplitude $A_{nk}(\infty)$ is written as

$$\begin{aligned}A_{nk}(\infty)=&\delta_{n0}\delta_{k0}-i\int_{-\infty}^{\infty}dt_1\langle n;k\mid\tilde{V}(t_1)\mid 0;0\rangle\\&+(-i)^2\sum_{n',k'}\int_{-\infty}^{\infty}dt_1\int_{-\infty}^{t_1}dt_2\langle n;k\mid\tilde{V}(t_1)\mid n';k'\rangle\langle n';k'\mid\tilde{V}(t_2)\mid 0;0\rangle\\&+(-i)^3\sum_{n',k'}\sum_{n'',k''}\int_{-\infty}^{\infty}dt_1\int_{-\infty}^{t_1}dt_2\int_{-\infty}^{t_2}dt_3\langle n;k\mid\tilde{V}(t_1)\mid n';k'\rangle\langle n';k'\mid\tilde{V}(t_2)\mid n'';k''\rangle\\&\times\langle n'';k''\mid\tilde{V}(t_3)\mid 0;0\rangle+\cdots\ .\end{aligned} \tag{2.15}$$

The right-hand side of the above equation is expressed as $\langle n;k\mid W(\infty,-\infty)\mid 0;0\rangle$, where the operator $W(\infty,-\infty)$ is

$$\begin{aligned}W(\infty,-\infty)=&E-i\int_{-\infty}^{\infty}dt\,\tilde{V}(t)+(-i)^2\int_{-\infty}^{\infty}dt_1\int_{-\infty}^{t_1}dt_2\tilde{V}(t_1)\tilde{V}(t_2)\\&+(-i)^3\int_{-\infty}^{\infty}dt_1\int_{-\infty}^{t_1}dt_2\int_{-\infty}^{t_2}dt_3\tilde{V}(t_1)\tilde{V}(t_2)\tilde{V}(t_3)+\cdots\\=&E-i\int_{-\infty}^{\infty}dt\tilde{V}(t)+(-i)^2/2!\int_{-\infty}^{\infty}dt_1\int_{-\infty}^{\infty}dt_2\mathscr{T}[\tilde{V}(t_1)\tilde{V}(t_2)]\\&+[(-i)^3/3!]\int_{-\infty}^{\infty}dt_1\int_{-\infty}^{\infty}dt_2\int_{-\infty}^{\infty}dt_3\mathscr{T}[\tilde{V}(t_1)\tilde{V}(t_2)\tilde{V}(t_3)]+\cdots\\=&\mathscr{T}\exp\left[-i\int_{-\infty}^{\infty}dt\,\tilde{V}(t)\right]\ ,\end{aligned} \tag{2.16}$$

since the $\langle n;k\mid$'s (or $\mid n:k\rangle$'s) form a complete set. In (2.16), $\mathscr{T}$ is the chronological ordering operator and E the unit operator.

Up to this point the theory is straightforward. It is, however, difficult to obtain any results without further approximations. Therefore, first we drop the chronological ordering operator in (2.16). Even at this stage it is still difficult to evaluate all of the matrix elements of the operator $\tilde{V}(t)$. Second, in evaluating the summation over intermediate states on the right-hand side of (2.15) or (2.16), we specifically include only such matrix elements $\langle i\mid\tilde{V}(t)\mid j\rangle$ for which either the bra or the ket vectors (i.e., $\langle i\mid$ or $\mid j\rangle$) is the ground state (i.e., $\langle 0;0\mid$ and $\mid 0;0\rangle$) and the other ket or bra is arbitrary. As we will see later, these approximations do not break the unitarity of the operator $W(\infty,-\infty)$ and consequently keep the total probability unity. Actually, under these conditions, the following expression for $A_{nk}(\infty)$ ($\mid n;k\rangle\neq\mid 0;0\rangle$) is obtained:

$$
\begin{aligned}
A_{nk}(\infty) = & -i\int_{-\infty}^{\infty} dt_1 \langle n;k \mid \tilde{V}(t_1) \mid 0;0\rangle \\
& + [(-i)^3/3!]\int\int\int_{-\infty}^{\infty} dt_1 dt_2 dt_3 \sum_{n',k'} \langle n;k \mid \tilde{V}(t_1) \mid 0;0\rangle\langle 0;0 \mid \tilde{V}(t_2) \mid n';k'\rangle\langle n';k' \mid \tilde{V}(t_3) \mid 0;0\rangle \\
& + [(-i)^5/5!]\int\int\int\int\int_{-\infty}^{\infty} dt_1 dt_2 dt_3 dt_4 dt_5 \sum_{n',k'}\sum_{n'',k''} \langle n;k \mid \tilde{V}(t_1) \mid 0;0\rangle\langle 0;0 \mid \tilde{V}(t_2) \mid n';k'\rangle \\
& \qquad \times \langle n';k' \mid \tilde{V}(t_3) \mid 0;0\rangle\langle 0;0 \mid \tilde{V}(t_4) \mid n'';k''\rangle \\
& \qquad \times \langle n'';k'' \mid \tilde{V}(t_5) \mid 0;0\rangle + \cdots \\
= & -i\int_{-\infty}^{\infty} dt_1 \langle n;k \mid \tilde{V}(t_1) \mid 0;0\rangle (1 - p_t/3! + p_t^2/5! + \cdots) \\
= & -i\int_{-\infty}^{\infty} dt_1 \langle n;k \mid \tilde{V}(t_1) \mid 0;0\rangle p_t^{-1/2} \sin(p_t^{1/2}) ,
\end{aligned}
\tag{2.17}
$$

where

$$
p_t = \sum_{n',k'} p_{n'k'}(b), \quad p_{n'k'}(b) = \left| \int_{-\infty}^{\infty} dt \langle n';k' \mid \tilde{V}(t) \mid 0;0\rangle \right|^2 . \tag{2.18}
$$

In (2.17) there are no matrix elements for even-order terms of $\tilde{V}(t)$. The reason is the following: if it were possible, they would have to include the factor such as $\langle 0;0 \mid \tilde{V}(t) \mid 0;0\rangle$ under the approximations considered. However, they cannot contribute since $\tilde{V}(t)$ has vanishing diagonal matrix elements.

On the other hand, the survival amplitude of the initial state, $A_{00}(\infty)$, is estimated as follows:

$$
\begin{aligned}
A_{00}(\infty) = & 1 + [(-i)^2/2!]\sum_{n',k'}\int\int_{-\infty}^{\infty} dt_1 dt_2 \langle 0;0 \mid \tilde{V}(t_1) \mid n';k'\rangle\langle n';k' \mid \tilde{V}(t_2) \mid 0;0\rangle \\
& + [(-i)^4/4!]\sum_{n',k'}\sum_{n'',k''}\int\int\int\int_{-\infty}^{\infty} dt_1 dt_2 dt_3 dt_4 \langle 0;0 \mid \tilde{V}(t_1) \mid n';k'\rangle\langle n';k' \mid \tilde{V}(t_2) \mid 0;0\rangle \\
& \qquad \times \langle 0;0 \mid \tilde{V}(t_3) \mid n'';k''\rangle\langle n'';k'' \mid \tilde{V}(t_4) \mid 0;0\rangle + \cdots \\
= & 1 - p_t/2! + p_t^2/4! + \cdots \\
= & \cos(p_t^{1/2}) .
\end{aligned}
\tag{2.19}
$$

In the case of $A_{00}(\infty)$, the matrix elements for odd-order terms of $\tilde{V}(t)$ cannot be incorporated into (2.19). Finally, we can get the transition probability to the $|n;k\rangle$ $(\neq |0;0\rangle)$ state and the survival probability of the $|0;0\rangle$ state in the forms

$$
\begin{aligned}
\mathscr{P}_{nk}(b) &= [p_{nk}(b)/p_t]\sin^2(p_t^{1/2}) , \\
\mathscr{P}_{00}(b) &= \cos^2(p_t^{1/2}) .
\end{aligned}
\tag{2.20}
$$

The total probability to find the electron in any $|n;k\rangle$ states is obtained by summing over n and k, and consequently the following can be proved:

$$
\begin{aligned}
\sum_{\substack{n,k \\ (n\neq 0 \text{ or } k\neq 0)}} \mathscr{P}_{nk}(b) + \mathscr{P}_{00}(b) &= \sin^2(p_t^{1/2}) + \cos^2(p_t^{1/2}) \\
&= 1 .
\end{aligned}
\tag{2.21}
$$

This shows conservation of probability, and we can see that the approximations adopted in the model here presented do not destroy the unitarity.

The approximation of dropping the $\mathscr{T}$ operator means that the limited sections of the time integral of the transition-matrix elements are extended over from $-\infty$ to ∞. Namely, the time-ordered multiple integral is replaced by the product of single integrals over independent time variables. It may not be easy to estimate quantitatively the extent to which the dropping of the $\mathscr{T}$ operator is valid, since the operator $W(\infty,-\infty)$ is composed of infinite power series of $\tilde{V}(t)$. However, as will be seen later, the formula (2.20) with (2.18) is equivalent to the first-order perturbation treatment if $p_t \ll 1$. Moreover, the present formulation actually ensures the conservation of probability. The expression (2.20) with (2.18), therefore, improves the first-order treatment, including the FBA.

The matrix elements $\langle n;k \mid \gamma(t) \mid n;k\rangle$ and $\langle n;k \mid V_{\text{int}}(t) \mid n;k\rangle$ in (2.12) indicate the distortion and the energy-level shift of the $|n;k\rangle$ state, respectively. The explicit form of $\langle n;k \mid V_{\text{int}}(t) \mid n;k\rangle$ is given as

$$\langle n;k \mid V_{\rm int}(t) \mid n;k\rangle = V_{1n}(\mathbf{R}) + V_{2k}(\mathbf{R}) + V_{nk}(\mathbf{R}) ,$$
$$V_{1n}(\mathbf{R}) = -\int d\mathbf{r}_1 Z_2 \mid \phi_n(\mathbf{r}_1)\mid^2 / \mid \mathbf{R}+\mathbf{r}_1 \mid ,$$
$$V_{2k}(\mathbf{R}) = -\int d\{\mathbf{r}_2\} Z_1 \mid \Psi_k(\{\mathbf{r}_2\})\mid^2 \sum_j 1/\mid \mathbf{R}-\mathbf{r}_{2j}\mid , \tag{2.22}$$
$$V_{nk}(\mathbf{R}) = \int\int d\mathbf{r}_1 d\{\mathbf{r}_2\} \times \sum_j \mid \phi_n(\mathbf{r}_1)\mid^2 \times \mid \Psi_k(\{\mathbf{r}_2\})\mid^2 / \mid \mathbf{R}+\mathbf{r}_1-\mathbf{r}_{2j}\mid ,$$

where $V_{1n}(R)$ $[V_{2k}(R)]$ denotes the energy-level shift of the electronic state n $[k]$ of a projectile [of a target atom] due to the field of a target nucleus [of a projectile nucleus] at the position R, and $V_{nk}(R)$ does the electron-electron interaction between n and k states. These energy-level-shift terms become significant as the impact velocity decreases. Actually the so-called Landau-Zener method, which corresponds to the stationary-phase method applied to the energy-level crossing, is a powerful tool to estimate the excitation cross sections in the low-impact-velocity cases $v \ll v_0$. Since we concentrate ourselves on the velocity range $v \gtrsim v_0$, the energy-level-shift terms can all be neglected.

For the electron-loss process, the ionization probability in (2.20) includes two contributions: one is from the elastic part ($k=0$), which means that the target atom remains in the ground state (i.e., $\mid 0;0\rangle$) in the ejection of the electron from the projectile, and the other is from the inelastic part ($k\neq 0$), for which the target atom is excited as well as the projectile. From a rough estimate using (2.18) on the basis of the first-order theory,[12] the inelastic contribution to the loss cross section is proportional to Z_2, while the elastic one is proportional to Z_2^2. Therefore except for small-Z_2 atoms, we may neglect the inelastic contribution in comparison with the elastic one. This treatment is also applied to the estimation of the excitation cross section using (2.20). Hereafter only the elastic part is taken into account. Then we are led to the following:

$$\langle n;k \mid \bar{V}(t) \mid 0;0\rangle \sim \langle n;0 \mid V_{\rm int}(t) \mid 0;0\rangle \exp(i\epsilon_{n0}^{(p)} t) = \int d\mathbf{r}_1 \phi_n^*(\mathbf{r}_1) \bar{V}(\mathbf{R}+\mathbf{r}_1) \times \phi_0(\mathbf{r}_1) \exp(i\epsilon_{n0}^{(p)} t) , \tag{2.23}$$

with

$$\epsilon_{n0}^{(p)} = \epsilon_n^{(p)} - \epsilon_0^{(p)} , \tag{2.24}$$

$$\bar{V}(\mathbf{R}+\mathbf{r}_1) = \left\langle 0 \left| -Z_2/\mid \mathbf{R}+\mathbf{r}_1\mid + \sum_j 1/\mid \mathbf{R}+\mathbf{r}_1-\mathbf{r}_{2j}\mid \right| 0 \right\rangle .$$

In the above, $\bar{V}(\mathbf{R}+\mathbf{r}_1)$ denotes the average potential of the target atom in the ground state at the position $\mathbf{R}+\mathbf{r}_1$, and $\epsilon_{n0}^{(p)}$ the energy difference between n and 0 states of the projectile. From (2.23) and (2.24), we easily recognize that the electron loss and excitation processes contributed from the elastic part are closely related with the average potential field of a target atom. These processes may therefore be called potential ionization and potential excitation, respectively.

Here we adopt as $\bar{V}$ in (2.24) the Molière potential in the form

$$\bar{V}(r) = -(Z_2/r)\chi(r/a_{\rm TF}) ,$$
$$\chi(x) = \sum_{i=1}^{3} \alpha_i \exp(-\beta_i x) , \tag{2.25}$$
$$a_{\rm TF} = 0.8853 Z_2^{-1/3} ,$$

where the parameters are given as $\{\alpha_1,\alpha_2,\alpha_3\} = \{0.10,0.55,0.35\}$ and $\{\beta_1,\beta_2,\beta_3\} = \{6.0,\ 1.2,\ 0.3\}$, and $a_{\rm TF}$ and $\chi(x)$ are the Thomas-Fermi (TF) screening length and the screening function, respectively. From Poisson's equation, the spatial electron distribution $\rho(r)$ in a target atom is obtained as

$$\rho(r) = -(1/4\pi)\Delta\bar{V}(r) \tag{2.26}$$

on the assumption that $\rho(r)$ is spherically symmetric. Applying the Fourier transform to $\rho(r)$, the form factor is found to be of the form

$$f_{00}(q) = Z_2 \sum_{i=1}^{3} \alpha_i / [1+(a_{\rm TF} q/\beta_i)^2] , \tag{2.27}$$

which is a scalar function of q $(=\mid \mathbf{q}\mid)$. The initial and final wave functions for the projectile-ionization process have the following form:

$$\phi_0(\mathbf{r}) = (\pi a_1^3)^{-1/2} \exp(-r/a_1), \quad a_1 = Z_1^{-1}$$
$$\phi_{\boldsymbol{\kappa}}(\mathbf{r}) = (2\pi)^{-3/2} \exp(i\boldsymbol{\kappa}\cdot\mathbf{r}) , \tag{2.28}$$

where a plane wave is used for simplification of further calculations.

Using the above wave functions and integrating the square of the absolute value of the transition-matrix element over the wave vector $\boldsymbol{\kappa}$ of the ejected electron, the quantity $p_i(b)$, i.e., $p_{n0}(b)$ in (2.18) for ionization process, is expressed in the form

$$p_i(b) = (2^6/\pi a_1^5 v^2) \times \int\int d\kappa_y \kappa_y d\kappa_z \times \sum_{m=0}^{\infty} h_m \left[\int_0^{\infty} dq_y q_y J_m(q_y b)(q_y^2+q_z^2)^{-1} [Z_2 - f_{00}(-\mathbf{q})] \left[\frac{(A^2-B^2)^{1/2}-A}{B} \right]^m [A/(A^2-B^2)^{3/2} + m/(A^2-B^2)] \right]^2 , \tag{2.29}$$

where

$$q=(q_y^2+q_z^2)^{1/2},\quad q_z=-(\epsilon_\kappa^{(p)}-\epsilon_0^{(p)})/v\ ,$$
$$\epsilon_\kappa^{(p)}=\tfrac{1}{2}(\kappa_y^2+\kappa_z^2),\quad \epsilon_0^{(p)}=-\tfrac{1}{2}a_1^{-2}\ , \tag{2.30}$$
$$A=a_1^{-2}+q_y^2+\kappa_y^2+(q_z-\kappa_z)^2,\quad B=2q_y\kappa_y\ .$$

In (2.29), $h_m=1$ for $m=0$ and $h_m=2$ for m a positive integer, and $J_m(q_yb)$ is the Bessel function of the mth order. The subscripts z and y denote the direction of motion of the projectile and the direction perpendicular to the z direction, respectively.

On the other hand, the quantity $p_{n0}(b)$, the probability of exciting the electron to the excited state n from the ground state 0 in the first-order theory, is calculated in the parabolic coordinates as follows:

$$p_{n0}(b)=(2/v)^2\sum\left|\int_0^\infty dq_yq_yJ_0(q_yb)(q_y^2+q_z^2)^{-1}\langle n\mid\exp(i\mathbf{q}\cdot\mathbf{r})\mid 0\rangle[Z_2-f_{00}(-\mathbf{q})]\right|^2, \tag{2.31}$$

with

$$\langle n\mid\exp(i\mathbf{q}\cdot\mathbf{r})\mid 0\rangle=2^4n^3Q[nQ-i(n_1-n_2)][(n^2-1)+n^2Q^2-i2nQ]^{n_1-1}$$
$$\times[(n^2-1)+n^2Q^2+i2nQ]^{n_2-1}/[(n+1)^2+n^2Q^2]^n\ , \tag{2.32}$$

where

$$Q=q/Z_1,\quad q=(q_y^2+q_z^2)^{1/2},\quad q_z=-(\epsilon_n^{(p)}-\epsilon_0^{(p)})/v,\quad \epsilon_n^{(p)}=-(1/2)a_1^{-2}/n^2\ \ (n=2,3,4,\ldots)\ . \tag{2.33}$$

In the above equations [(2.31)–(2.33)], n is the principal quantum number connected with the other quantum number n_1 and n_2 through the relation $n_1+n_2+1=n$ $(n_1,n_2=0,1,2,\ldots,n-1)$. Therefore, $\sum$ in (2.31) means the summation over an integer n_1 (or n_2) from 0 to $n-1$. Since $n=1$ is a label for the ground state, $n\geqq 2$ are assigned to the excited states.

Rewriting $p_{nk}(b)$ in (2.18) and (2.20), the electron-loss and excitation probabilities as a function of impact parameter b are given as

$$\mathscr{P}_i(b)=[p_i(b)/p_t(b)]\sin^2[p_t(b)^{1/2}]\ ,$$
$$\mathscr{P}_{n0}(b)=[p_{n0}(b)/p_t(b)]\sin^2[p_t(b)^{1/2}]\ , \tag{2.34}$$

with

$$p_t(b)=p_i(b)+\sum_{n=2}^{n_c}p_{n0}(b)\ , \tag{2.35}$$

where n_c is an appropriate cut-off integer for simplification of the numerical evaluation. The electron-loss and excitation cross sections are given as

$$\sigma_{\text{loss}}=2\pi\int_0^\infty db\,b\,\mathscr{P}_i(b)\ ,$$
$$\sigma_{n0}=2\pi\int_0^\infty db\,b\,\mathscr{P}_{n0}(b)\ . \tag{2.36}$$

For relatively large impact parameters, the inequality $p_t(b)\ll 1$ is satisfied. Then Eqs. (2.34) and (2.35) reduce the first-order theory:

$$\mathscr{P}_i(b)=p_i(b),\quad \mathscr{P}_{n0}(b)=p_{n0}(b)\ . \tag{2.37}$$

Generally this condition is also satisfied over all impact parameters at impact velocities much higher than the orbital velocity of the ejected electron. Inserting (2.37) into

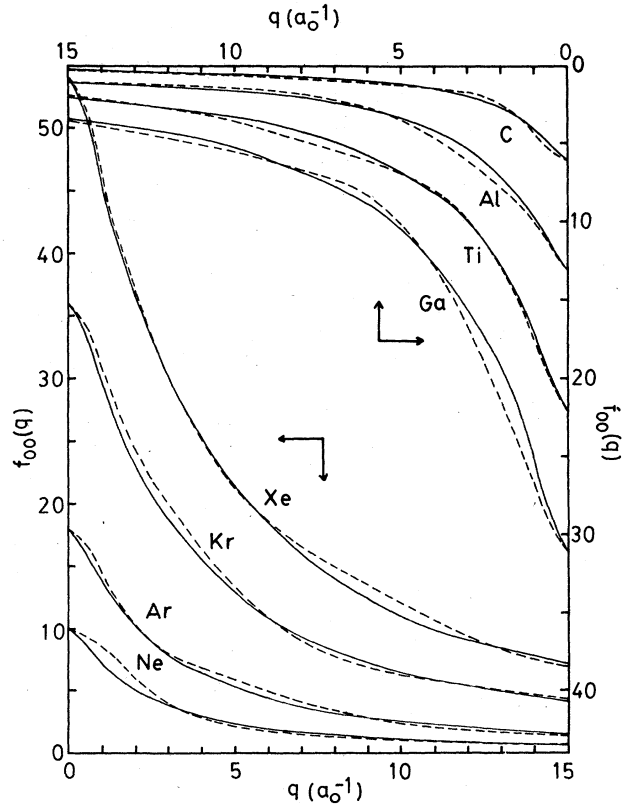

FIG. 2. The atomic form factors $f_{00}(q)$ for C, Ne, Al, Ar, Ti, Ga, Kr, and Xe atoms derived from the Molière electron distribution (——) and from the Hartree-Fock wave functions (Ref. 13, ---). Arrows indicate the scale of the vertical and the horizontal axes.

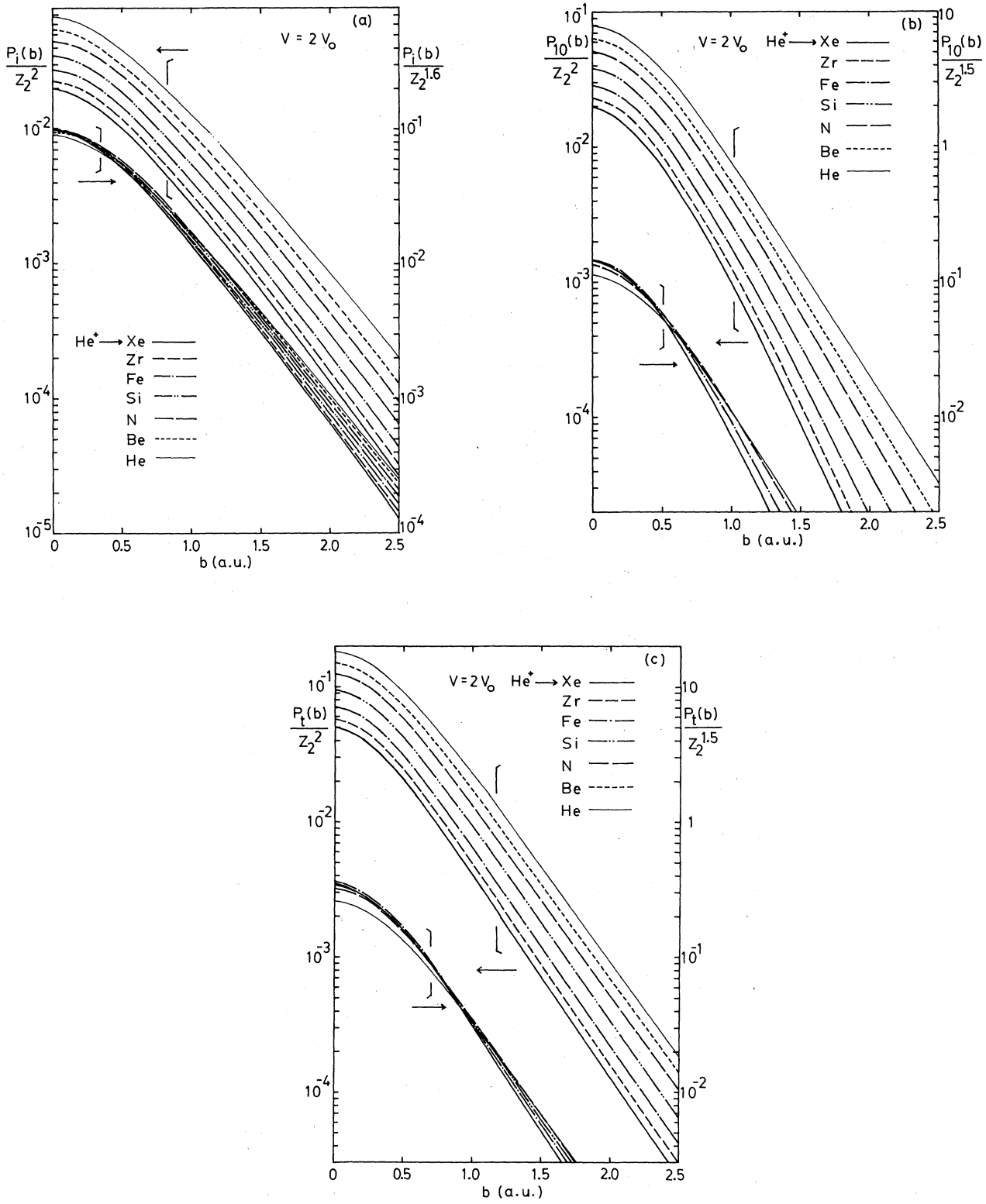

FIG. 3. The quantities $p_i(b)$, $p_{10}(b)$, and $p_t(b)$ as functions of the impact parameter b in the case of a He^+ ion incident on He, Be, N, Si, Fe, Zr, and Xe atoms at $v = 2v_0$. The arrows indicate the scale of the vertical axis.

(2.36), we obtain the cross sections based on the first-order theory, corresponding to the FBA.

III. NUMERICAL RESULTS AND DISCUSSIONS

First the atomic form factor $f_{00}(q)$, which appears in (2.27), is illustrated in Fig. 2 for C, Ne, Al, Ar, Ti, Ga, Kr, and Xe target atoms. As is easily seen, the form factors derived from the Molière electron distribution (MED) in (2.25) are very close to those from the numerical tables[13] of the Hartree-Fock wave functions. In the latter case the spatial electron distribution is spherically averaged in our calculation. Figure 2 indicates that the MED is fully useful and sufficient to describe the form factors for neutral atoms in spite of its simple analytical form.

In Figs. 3(a)—3(c), the quantities $p_i(b)$, $p_{10}(b)$ [hereafter the subscript 1 in $p_{10}(b)$ and σ_{10} denotes the first excited state ($n=2$)], and $p_t(b)$ are drawn as functions of the impact parameter b for a He^+ ion colliding with He, Be, N, Si, Fe, Zr, and Xe target atoms at the impact velocity $v=2v_0$. Each of them falls off nearly exponentially with respect to b except for small impact parameters. For large Z_2 numbers, $p_i(b)$ behaves not as $\sim Z_2^2$ but as $\sim Z_2^{1.6}$, and both $p_{10}(b)$ and $p_t(b)$ do as $\sim Z_2^{1.5}$. This feature is due to the fact that the target electrons screen the electric field of the target nucleus. It is clearly seen that $p_i(b)$ and $p_{10}(b)$, and consequently $p_t(b)$, exceed unity in a small impact-parameter region for large-Z_2 atoms. This directly reveals that the first-order theory breaks down there, while in our approximation there is no breakdown. We set $n_c=10$, which is enough to estimate the summation over n in (2.35), judging from the usual n^{-3} rule,[9] such as $|\langle n|\exp(i\mathbf{q}\cdot\mathbf{r})|0\rangle|^2\sim n^{-3}$ for large n. In summation over m in (2.29), only the contribution from $m=0$ is evaluated since it is dominant. In a first-order theory, $p_{nk}(b)$ in (2.18) is regarded as the transition probability as a function of impact parameter, whether or not is exceeds unity. Then the velocity dependence of the electron-loss and excitation cross sections is described as $\sim v^{-2}$ for $v\gg v_c$, where v_c is the ion velocity at which the cross section amounts to be a maximum for a given target material. This velocity dependence is consistent with the characteristic of the corresponding cross section in the FBA. It is found that in Figs. 3(a)—3(c), each of the curves of $p_1(b)$, $p_{10}(b)$, and $p_t(b)$ tend to converge into a common curve, respectively, for large Z_2. Even at other impact velocities, the feature of both the exponential decrease with b and the Z_2 dependences of $p_i(b)$, $p_{10}(b)$, and $p_t(b)$ will not be so different from those at $v=2v_0$.

From the above three quantities, the electron-loss and excitation probabilities, i.e., $\mathscr{P}_i(b)$ and $\mathscr{P}_{10}(b)$, are obtained from (2.34). In Fig. 4, $\mathscr{P}_i(b)$ and $\mathscr{P}_{10}(b)$ are drawn for a He^+ ion incident on Ar atoms at $v=2v_0$. As is naturally expected from (2.34), both probabilities have the same phase of oscillation although their amplitudes are different from each other. The quantity $p_{10}(b)$ falls off more rapidly than $p_i(b)$ with increasing b so that the envelope function of $\mathscr{P}_{10}(b)$, i.e., $p_{10}(b)/p_t(b)$, decreases with b and conversely that of $\mathscr{P}_i(b)$, i.e., $p_i(b)/p_t(b)$, increases with b.

In Figs. 5—8, the energy dependences of the electron-loss cross sections for a He^+ ion colliding with He, N_2, Ar, and Kr atoms are shown. In the case of the N_2 target, the molecular effect is ignored so that the cross section is obtained by multiplying that for a N atom by a factor of 2. From these figures, good agreements with the experimental data[14–18] are obtained over a wide impact-energy region for He, N_2, and Ar targets, while for Kr atoms, theory yields quantitatively significant differences in the energy range of $E\lesssim 1$ MeV. As will be seen later, the calculated loss cross sections show a slowly increasing tendency with increasing Z_2 number. The experimental data, however, give smaller cross sections for Kr ($Z_2=36$) atoms than for Ar ($Z_2=18$) atoms at the energies $E\lesssim 1$ MeV. This discrepancy cannot be understood reasonably for the moment. It should be noted that for a He target atom the form factor derived from the MED will be underestimated so that the calculated loss cross section will be overestimated a bit. Following from the numerical estimation, $\sigma_{\text{loss}}\sim E^{2.8}$ in the energy range of $30\lesssim E\lesssim 150$ keV for He, N_2, Ar, and Kr atoms, where no

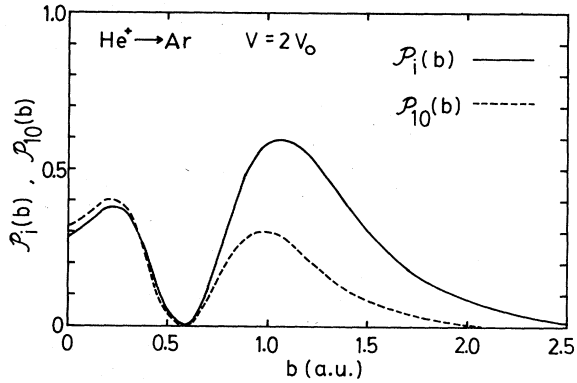

FIG. 4. Electron-loss and the excitation probabilities, $\mathscr{P}_i(b)$ and $\mathscr{P}_{10}(b)$, as a function of the impact parameter b for a He^+ ion colliding with an Ar target at $v=2v_0$.

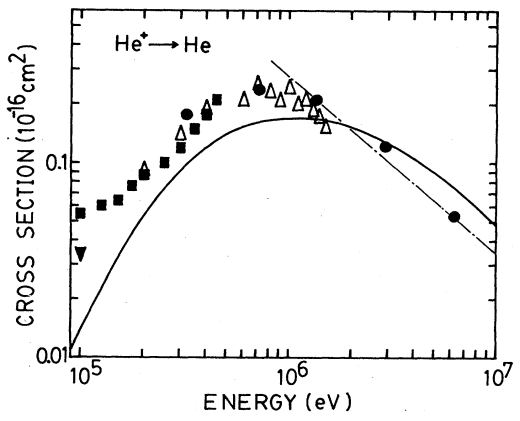

FIG. 5. Energy dependence of the electron-loss cross section for a He^+ ion colliding with He target: the present theory (——) and the experiments (△, Ref. 14; ■, Ref. 15; ●, Ref. 16; ▼, Ref. 17). —·— is FBA results by Dmitriev (Ref. 16).

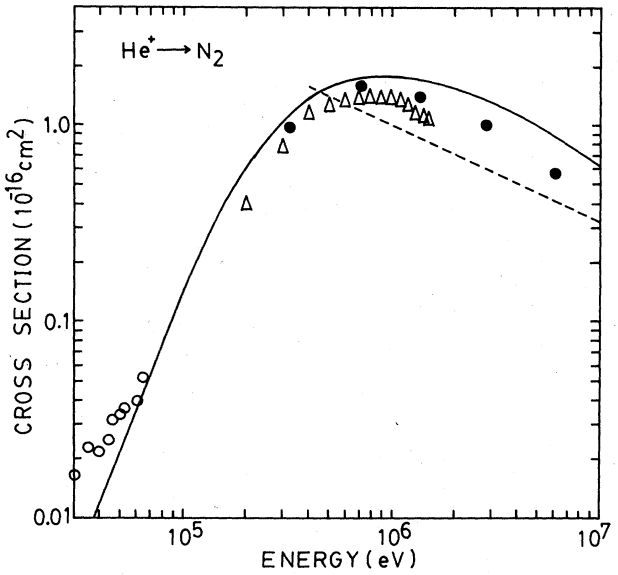

FIG. 6. Same as in Fig. 5 except for N_2 target: the present theory (——) and the experiments (△, Ref. 14; ●, Ref. 16; ○, Ref. 18). — — —, Bohr formula (1.1).

remarkable differences in the energy dependence of σ_{loss} can be found for any Z_2 material. On the other hand, in the range of $4 \lesssim E \lesssim 10$ MeV, the material dependence appears in the power index of energy such that $\sigma_{\text{loss}} \sim E^{-1}$ for He, $\sim E^{-0.64}$ for N_2, $\sim E^{-0.44}$ for Ar, and $\sim E^{-0.36}$ for Kr target. As far as the He target is concerned, the

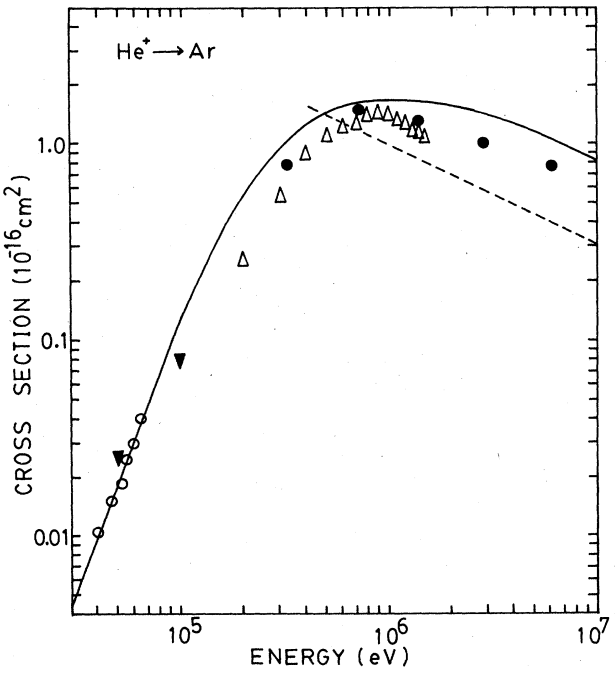

FIG. 7. Same as in Fig. 6 except for Ar target: the experiments (△, Ref. 14; ●, Ref. 16; ▼, Ref. 17; ○, Ref. 18).

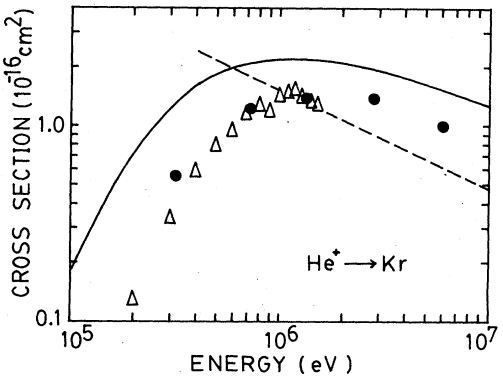

FIG. 8. Same as in Fig. 6 except for Kr target: the experiments (△, Ref. 14; ●, Ref. 16).

FBA yields the same E^{-1} energy dependence. Following Bohr, σ_{loss} is proportional to $E^{-0.5}$ regardless of Z_2 for $v > Z_1 v_0$ in the free-collision approximation. Then his result is, as a whole, close to ours for heavy target atoms. However, our calculations present a weak Z_2 dependence in the power index of energy, where the absolute value of the power becomes small with increasing Z_2 number. This recommends a weaker Z_2 dependence of the loss

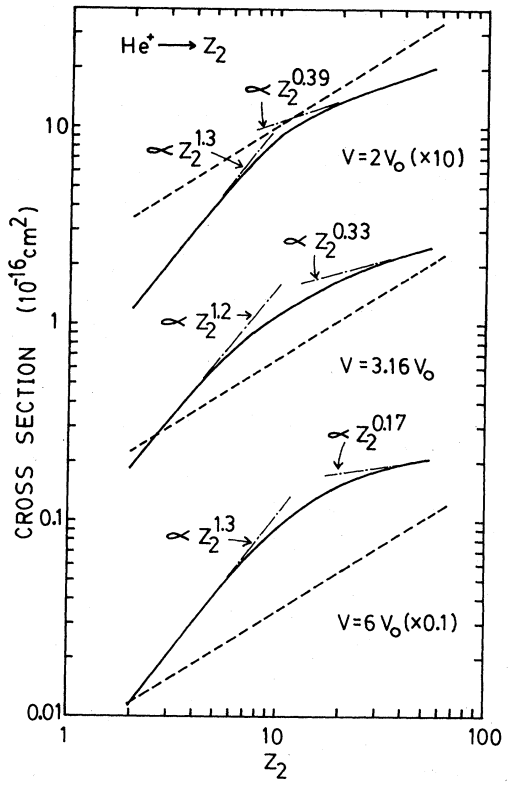

FIG. 9. Electron-loss cross section for a He^+ ion with respect to Z_2 at $v = 2v_0$, $3.16v_0$, and $6v_0$. Solid lines and the dashed lines denote the present results and Bohr's, respectively. —·— show the asymptotic behaviors.

cross sections than the Bohr formula. It is worthwhile to compare the velocity v_c predicted by this theory with that by the first-order theory. Based on the first-order theory or the FBA, v_c is nearly equal to $Z_1 v_0$ ($=2v_0$ for a He^+ ion) for the electron-loss process, while our theory indicates that v_c is approximately twice as large as $2v_0$. This noticeable difference is distinguished experimentally,[14,16] supporting our prediction. As far as the excitation cross section σ_{10} is concerned, it tends to be proportional to E^{-1} for He target at the impact energies ranging from 10^5 to 10^7 eV. However, for large-Z_2 materials, the absolute value p (>0) of the power of energy, where we assume $\sigma_{10} \sim E^{-p}$, becomes smaller than unity and, for example, is reduced to 0.5 for the Xe ($Z_2=54$) target. As we have already seen, there exists a remarkable contrast between our theory and the first-order theory including the FBA in the energy dependences of the cross section σ_{loss} and σ_{10}.

Another conspicuous feature is shown in Figs. 9 and 10, where σ_{loss} and σ_{10} with respect to Z_2 ranging from 2 to 55 are illustrated at $v=2v_0$ (100 keV/amu), $3.16v_0$ (250 keV/amu), and $6v_0$ (900 keV/amu) with the experimental data[14,19] at $v=3.16v_0$. Bohr says $\sigma_{\text{loss}} \sim Z_2^{2/3}$ so that the log-log plots are on a straight line as is shown in Fig. 9. In our case, however, a weaker Z_2 dependence than Bohr's is found in the large-Z_2 region such that $\sigma_{\text{loss}} \sim Z_2^{0.39}$ at $v=2v_0$, $\sim Z_2^{0.33}$ at $v=3.16v_0$, and $\sim Z_2^{0.17}$ at $v=6v_0$. This result cannot be obtained by only taking into account the screening effect by the target electrons. Our result is consistent with the trend of the experimental data recently obtained by Dmitriev *et at.*[7] The excitation cross section σ_{10} for a He^+ ion, which is estimated from the envelope curve of $\mathscr{P}_{10}(b)$, displays a noteworthy Z_2 dependence as shown in Fig. 10, in which σ_{10} becomes constant for $Z_2 \gtrsim 20$ and it represents a weaker Z_2 dependence rather than σ_{loss}. In order to confirm this dependence, a further calculation was performed for 40-MeV F^{8+} ions colliding with He, Ne, Ar, and Kr targets. As a result, the theory yields good agreement with the data obtained by Kawatsura *et al.*,[20] in the measurement of the projectile x-ray production cross sections, as is shown in Fig. 11. Their experiment indirectly supports our calculation of σ_{10} for a He^+ ion, even if a different projectile was used. The only important condition is that it be hydrogen like. It is noted that the excitation cross sections excited states higher than the first are negligible in comparison with σ_{loss} and σ_{10}, since we have confirmed $\sigma_{n0}(n \geq 3) \sim n^{-2.3}\sigma_{10}$ at most. If we are allowed to use the Molière electron distribution for target atoms with $Z_2 > 55$, the cross sections considered here for electron-loss and excitation processes are straightforwardly obtained.

In conclusion, the unitarized impact-parameter method has greatly improved the first-order theory. Our procedure yields more consistent agreements with the experimental data by evaluating the interaction matrix elements to infinite order in spite of dropping the $\mathscr{T}$ operator. The electron-loss and excitation probabilities obtained here reproduce the shape and magnitude of the corresponding cross sections measured for a He^+ ion both over the impact energies ranging from ~ 30 to 10^4 keV and over the

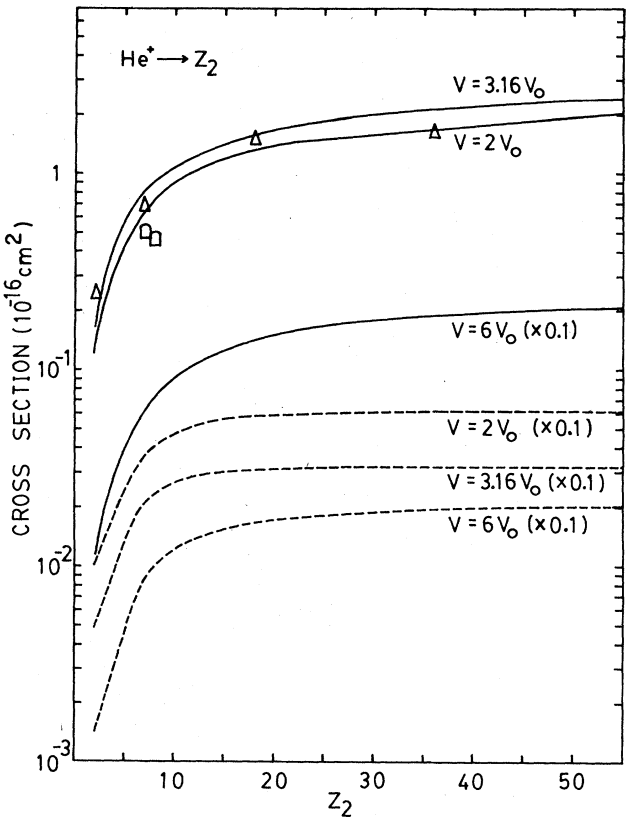

FIG. 10. Electron-loss and the excitation cross sections, σ_{loss} and σ_{10}, for a He^+ ion with respect to Z_2: the present results (—— for σ_{loss} and — — — for σ_{10}) at $v=2v_0$, $3.16v_0$, and $6v_0$ and the experimental results (△, Ref. 14; □, Ref. 19) at $v=3.16v_0$.

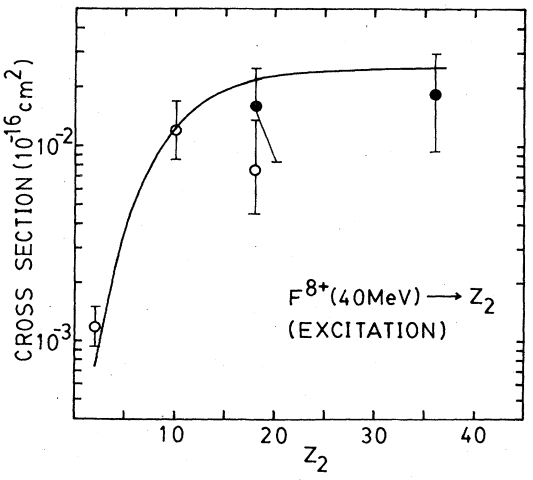

FIG. 11. Excitation cross section for 40-MeV F^{8+} ions with respect to Z_2: the theory (——) and the experiment by Kawatsura *et al.* (Ref. 20), where they extrapolated ⧗ from the results of Hopkins *et al.* (Ref. 21).

Z_2 number from 2 to 55. Our loss cross sections are found to increase less with respect to Z_2 for large Z_2 numbers than are Bohr's at the impact energies considered. The ion velocity, at which the loss cross section becomes a maximum for a given target, is estimated to be about twice as large as the orbital velocity of the ionized electron. The cross sections for exciting to the first excited state from the ground state of a He^+ ion are saturated with increasing Z_2 number. From the physical point of view, our procedure developed in this paper is interpreted as follows: on account of including the intermediate transitions between orthonormal states to all order terms of the interaction Hamiltonian, the amplitude of the survival probability of the initial state is effectively modified before transition to $p_t^{-1/2}\sin(p_t^{1/2})$. In the first-order theory or the FBA, this amplitude remains unity all over the time in contrast to our result. Finally it should be stressed that conclusions arise directly from the derived formula.

ACKNOWLEDGMENTS

The author would like to express his thanks to Professor Y. Yamamura for useful discussions. His sincere thanks are given to Dr. K. Kawatsura, Dr. P. Richard, and Dr. P. L. Pepmiller for their permission to refer to their data prior to publication. This work was financially supported by a Grant-in-Aid for Fundamental Scientific Research from the Ministry of Education, Japan, and also supported in part by Institute of Plasma Physics at Nagoya University, Japan.

[1]H.-D. Betz, Rev. Mod. Phys. **44**, 465 (1977), and in *Methods of Experimental Physics* (Academic, New York, 1980), Vol. 17, p. 73.

[2]N. E. B. Cowern, P. M. Read, C. J. Sofield, L. B. Bridwell, G. Huxtable, M. Miller, and M. W. Lucas, Nucl. Instrum. Methods Phys. Res. B **2**, 112 (1984).

[3]F. Besenbacher, J. U. Andersen, and E. Bonderup, Nucl. Instrum. Methods **168**, 1 (1980).

[4]J. F. Ziegler, in *The Stopping and Ranges of Ions in Matter,* edited by J. F. Ziegler (Pergamon, New York, 1977), Vol. 4.

[5]T. Kaneko, Phys. Rev. A **30**, 1714 (1984).

[6]Y. Haruyama, Y. Kanamori, T. Kido, and F. Fukuzawa, J. Phys. B **15**, 779 (1982); Y. Haruyama, Y. Kanamori, T. Kido, A. Itoh, and F. Fukuzawa, *ibid.* **16**, 1225 (1983).

[7]I. S. Dmitriev, N. F. Vorobiev, V. P. Zaikov, V. S. Nikolaev, and Ya.A. Teplova, J. Phys. B **15**, L351 (1982).

[8]T. Kaneko and Y. H. Ohtsuki, Phys. Status Solidi B **111**, 491 (1982).

[9]G. H. Gillespie, Phys. Rev. A **18**, 1967 (1978).

[10]D. W. Rule, Phys. Rev. A **16**, 19 (1977).

[11]N. Bohr, K. Dan. Vidensk. Selsk. Mat. Fys. Medd. **18**, No. 8 (1948).

[12]In neglecting the probability contributed from the inelastic part, our judgment is based on the cross section obtained from (2.36) within the first-order theory. The linear dependence of the cross section on Z_2 can be also derived from the FBA.

[13]E. Clementi and C. Roetti, At. Data Nucl. Data Tables **14**, 177 (1974).

[14]L. I. Pivovar, M. T. Novikov, and V. M. Tabaev, Zh Eksp. Teor. Fiz. **41**, 26 (1961) [Sov. Phys.—JETP **14**, 20 (1962)].

[15]S. K. Allison, Rev. Mod. Phys. **30**, 1137 (1958).

[16]I. S. Dmitriev, V. S. Nikolaev, L. N. Fateeva, and Ya.A. Teplova, Zh. Eksp. Teor. Fiz. **42**, 16 (1962) [Sov. Phys.—JETP **15**, 11 (1962)].

[17]P. R. Jones, F. B. Ziemba, H. A. Moses, and E. Everhart, Phys. Rev. **113**, 182 (1959).

[18]M. B. Shah and H. B. Gilbody, J. Phys. B **8**, 372 (1975).

[19]A. Itoh, K. Ohnishi, and F. Fukuzawa, J. Phys. Soc. Jpn. **49**, 1513 (1980).

[20]K. Kawatsura, P. Richard, and P. L. Pepmiller (private communication).

[21]F. Hopkins, R. Brenn, A. R. Whittemore, N. Cue, V. Dutkiewicz, and R. P. Chaturvedi, Phys. Rev. A **13**, 74 (1976).